

The architecture of an intrusion in a magmatic mush

Alexandre Carrara^{1*}, Alain Burgisser¹, George Bergantz²

¹ Univ. Grenoble Alpes, Univ. Savoie Mont Blanc, CNRS, IRD, IFSTTAR, ISTerre, 38000 Grenoble

² Department of Earth and Space Sciences, Box 351310, University of Washington, Seattle, WA, 98195, USA

* contact : carrara.alexandre.univ@gmail.com

Introduction

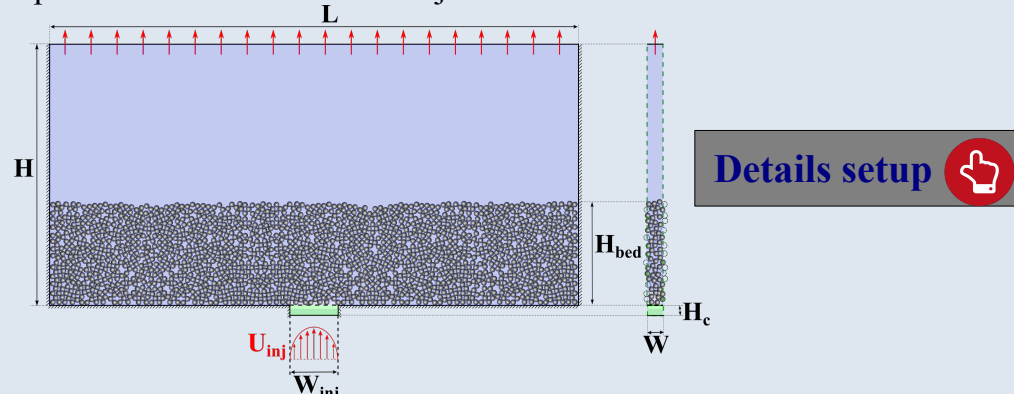
Magmatic reservoirs located in the upper crust have been shown to result from the repeated intrusions of new magmas, and spend much of the time as a crystal-rich mush. The geometry of the intrusion of new magmas may greatly affect the thermal and compositional evolution of the reservoir. Despite advances in our understanding of the physical processes that may occur in a magmatic reservoir, the resulting architecture of the composite system remains poorly constrained. Here we present numerical simulations to illuminate the geometry and emplacement dynamics of a new intrusion into mush and the relevant physical parameters controlling it.

Method

We performed CFD-DEM simulations based on MFIX-DEM (<https://mfix.netl.doe.gov/>) by varying the physical properties (density and viscosity) of host melt and injection velocity. All other parameters were kept constant.

Overview numerical method

The simulation domain is a box filled with a viscous fluid in which a particle bed of thickness H_{bed} is settled to mimic a magmatic mush layer. A melt having different properties than the host one is injected at the base of the tank.



Simulations were compared as a function of the following dimensionless quantities:

$$\eta^* = \frac{\eta(h)}{\eta(i)} \quad \text{Reduced melt density} \quad \rho^* = \frac{\rho(i) - \rho(h)}{\rho(i)} \quad \text{Reduced bulk density} \quad \rho_b^* = \frac{\rho(i) - [(1-\phi)\rho(h) + \phi\rho_c]}{\rho(i)}$$

Dimensionless injection velocity

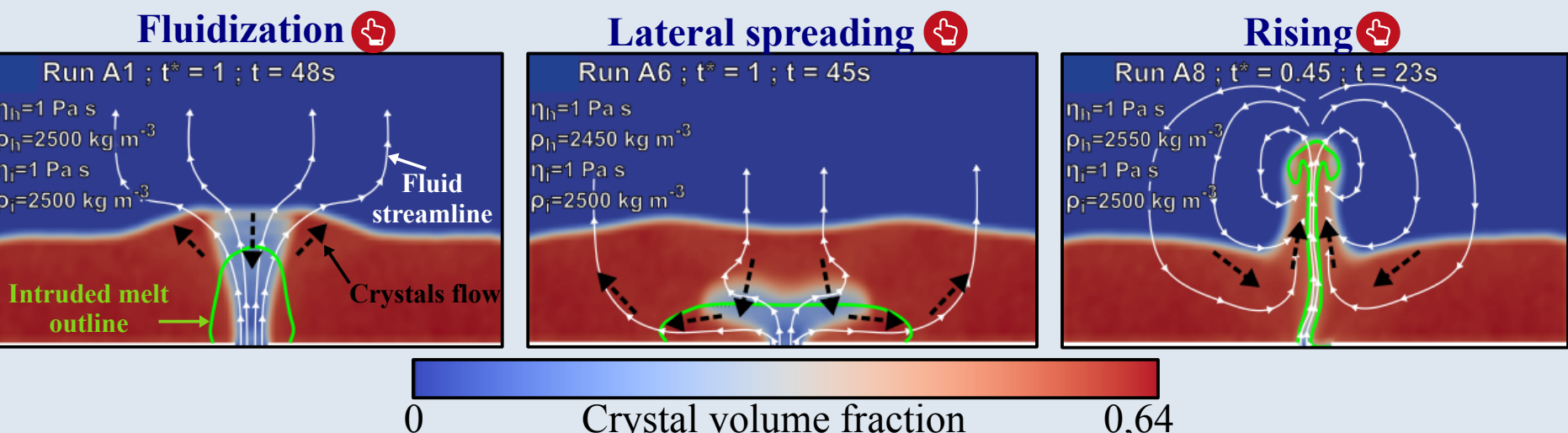
$$U^* = \frac{U_{inj}}{U_{mf}} \quad t^* = \frac{t U_{inj}}{H_{bed}}$$

Details on dimensionless quantities

- $\eta(h)$ = host melt viscosity
- $\eta(i)$ = intrusion melt viscosity
- $\rho(i)$ = intrusion melt density
- $\rho(h)$ = host melt density
- ρ_c = crystals density
- Φ = crystal volume fraction
- U_{inj} = injection velocity
- U_{mf} = minimum fluidization velocity
- t = dimensional time
- H_{bed} = Mush layer thickness

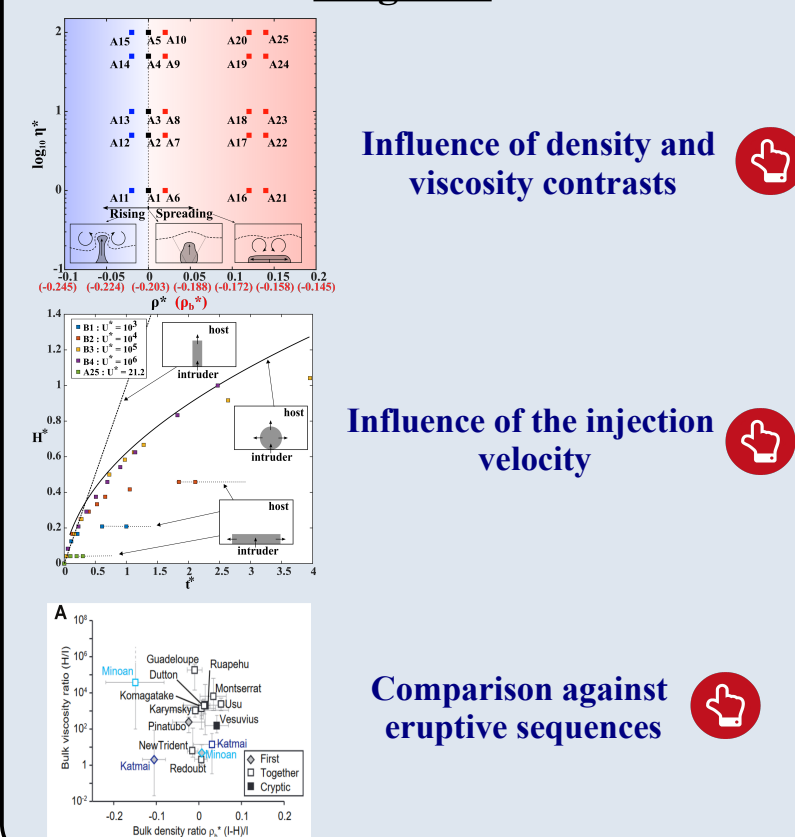
Simulation parameters

Intrusion regimes



Results

Diagrams



Summary of the results

- The density contrast between the two melt phases has a first order control on the emplacement mechanism and geometry of an intrusion in a mush.
- On the contrary, the bulk density contrast has no control on the intrusion style.
- The viscosity contrast and injection velocity do not directly control the intrusion geometry but exert a second order controls on the emplacement mechanism.
- The comparison against eruptive sequences shows a good agreement with the numerical results and illustrates the primary control exerted by the density contrast existing between the host and intruded melt phases.
- These results illustrate the importance of considering granular mechanisms when studying magmatic processes rather than straightforward assumptions as the bulk density contrast.

Conclusions

The geometry and emplacement mode of an intrusion in a magmatic mush are controlled primarily by the density contrast between the melt phases of the two end-member materials. The injection velocity and viscosity contrast appear to exert second order controls. These results illustrate the importance of granular mechanisms in magmatic processes. In most of the natural conditions, the intruded melt is denser than the host one, which results in the emplacement of the intrusion as an horizontal layer. More information at: <https://eartharxiv.org/hc4px>

Back to main slide



Parameter	Value or range
ρ_c	3300 kg m ⁻³
dp	4.5-5.5 mm
Nb crystals	208495
H_{bed}	0.3 m
W_{inj}	0.1 m
$\rho_m(i)$	2500 kg m ⁻³
$\eta(i)$	1 Pa s
E	2 10 ⁷ Pa
σ	0.32
μ	0.3

Table 1: Constant parameters used in the simulations

ρ_c	= Crystal density
dp	= crystal diameters
H_{bed}	= Mesh layer thickness
W_{inj}	= Injection width
$\rho(i)$	= melt density in the intrusion
$\eta(i)$	= Viscosity of the melt phase in the intrusion
E	= Crystal Young modulus
σ	= Crystal Poisson coefficient
μ	= Crystal friction coefficient
$\rho(h)$	= Host melt density
$\rho_b(i)$	= Bulk density of the host mush
ρ^*	= Melt reduced density
ρ_b^*	= Bulk reduced density
η^*	= Dimensionless viscosity contrast
U_{mf}	= Minimum fluidization velocity
U_{inj}	= Injection velocity

Run n°	$\rho_m(h)$	$\rho_b(h)$	ρ^*	ρ_b^*	η^*	U_{mf}	U_{inj}
A1	2500	3012	0	-0.2048	1	2.956 10 ⁻⁴	6.268 10 ⁻³
A2	2500	3012	0	-0.2048	5	5.913 10 ⁻⁵	1.254 10 ⁻³
A3	2500	3012	0	-0.2048	10	2.957 10 ⁻⁵	6.268 10 ⁻⁴
A4	2500	3012	0	-0.2048	50	5.913 10 ⁻⁶	1.254 10 ⁻⁴
A5	2500	3012	0	-0.2048	100	2.957 10 ⁻⁶	6.268 10 ⁻⁵
A6	2450	2994	0.02	-0.1976	1	3.141 10 ⁻⁴	6.660 10 ⁻³
A7	2450	2994	0.02	-0.1976	5	6.283 10 ⁻⁵	1.332 10 ⁻³
A8	2450	2994	0.02	-0.1976	10	3.141 10 ⁻⁵	6.660 10 ⁻⁴
A9	2450	2994	0.02	-0.1976	50	6.283 10 ⁻⁶	1.332 10 ⁻⁴
A10	2450	2994	0.02	-0.1976	100	3.141 10 ⁻⁶	6.660 10 ⁻⁵
A11	2550	3030	-0.02	-0.212	1	2.772 10 ⁻⁴	5.876 10 ⁻³
A12	2550	3030	-0.02	-0.212	5	5.544 10 ⁻⁵	1.175 10 ⁻³
A13	2550	3030	-0.02	-0.212	10	2.772 10 ⁻⁵	5.876 10 ⁻⁴
A14	2550	3030	-0.02	-0.212	50	5.544 10 ⁻⁶	1.175 10 ⁻⁴
A15	2550	3030	-0.02	-0.212	100	2.772 10 ⁻⁶	5.876 10 ⁻⁵
A16	2200	2904	0.12	-0.1616	1	4.065 10 ⁻⁴	8.618 10 ⁻³
A17	2200	2904	0.12	-0.1616	5	8.130 10 ⁻⁵	1.724 10 ⁻³
A18	2200	2904	0.12	-0.1616	10	4.065 10 ⁻⁵	8.618 10 ⁻⁴
A19	2200	2904	0.12	-0.1616	50	8.130 10 ⁻⁶	1.724 10 ⁻⁴
A20	2200	2904	0.12	-0.1616	100	4.065 10 ⁻⁶	8.618 10 ⁻⁵
A21	2150	2886	0.14	-0.1544	1	4.250 10 ⁻⁴	9.010 10 ⁻³
A22	2150	2886	0.14	-0.1544	5	8.500 10 ⁻⁴	1.802 10 ⁻³
A23	2150	2886	0.14	-0.1544	10	4.250 10 ⁻⁵	9.010 10 ⁻⁴
A24	2150	2886	0.14	-0.1544	50	8.500 10 ⁻⁶	1.802 10 ⁻⁴
A25	2150	2886	0.14	-0.1544	100	4.250 10 ⁻⁶	9.010 10 ⁻⁵
B1	2150	2886	0.14	-0.1544	100	4.250 10 ⁻⁶	4.250 10 ⁻³
B2	2150	2886	0.14	-0.1544	100	4.250 10 ⁻⁶	4.250 10 ⁻²
B3	2150	2886	0.14	-0.1544	100	4.250 10 ⁻⁶	4.250 10 ⁻¹
B4	2150	2886	0.14	-0.1544	100	4.250 10 ⁻⁶	4.250 10 ⁰

Table 2: Variable parameters used in the set of simulations. Simulation labeled with A explore the importance of the density and viscosity contrasts. Simulation labeled with B explore the influence of the injection velocity.

[Back](#)

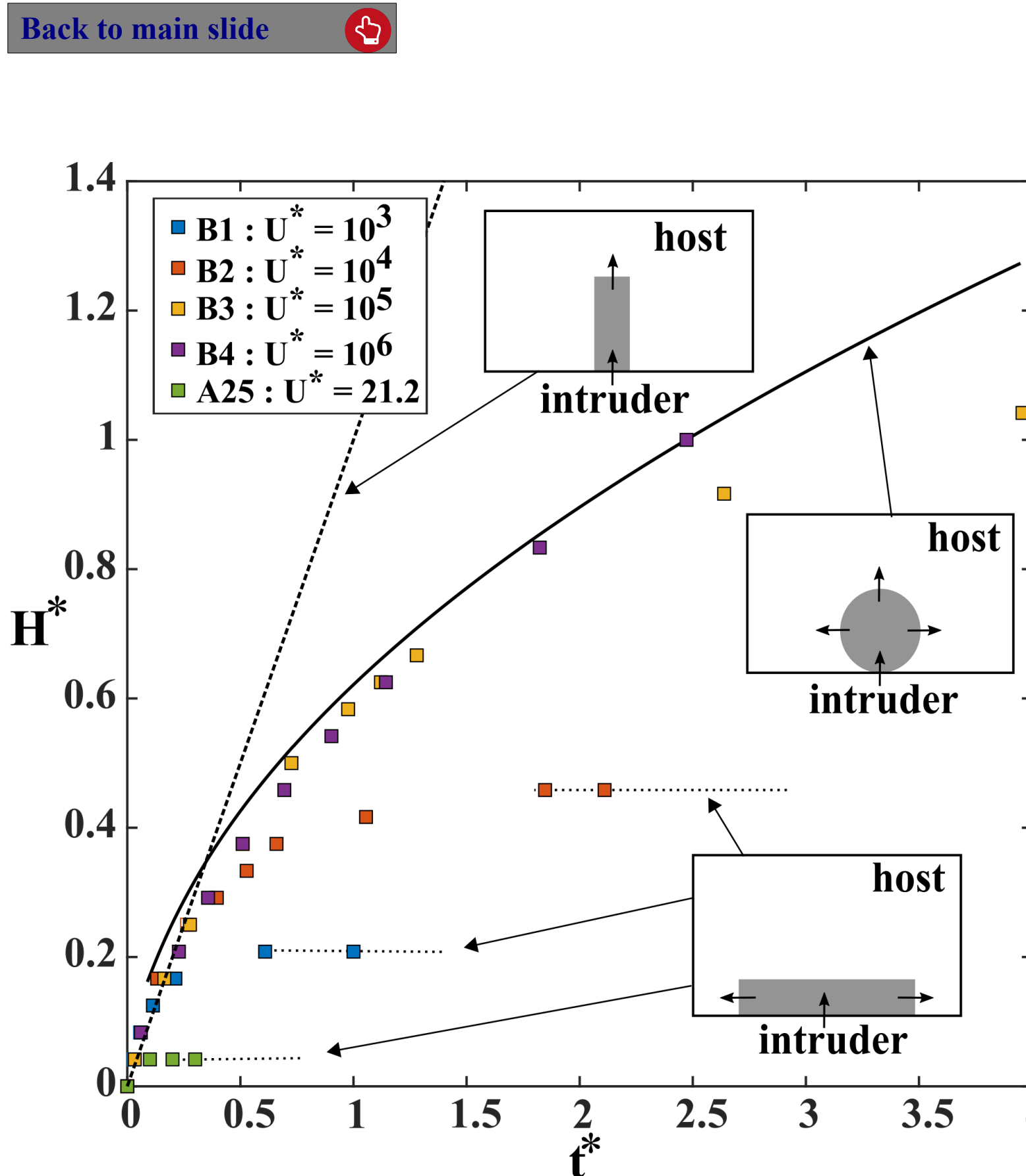
Parameter	Value or range
ρ_c	3300 kg m ⁻³
dp	4.5-5.5 mm
Nb crystals	208495
H_{bed}	0.3 m
W_{inj}	0.1 m
$\rho_m(i)$	2500 kg m ⁻³
$\eta(i)$	1 Pa s
E	2 10 ⁷ Pa
σ	0.32
μ	0.3

Table 1: Constant parameters used in the simulations

ρ_c	= Crystal density
dp	= crystal diameters
H_{bed}	= Mesh layer thickness
W_{inj}	= Injection width
$\rho(i)$	= melt density in the intrusion
$\eta(i)$	= Viscosity of the melt phase in the intrusion
E	= Crystal Young modulus
σ	= Crystal Poisson coefficient
μ	= Crystal friction coefficient
$\rho(h)$	= Host melt density
$\rho_b(i)$	= Bulk density of the host mush
ρ^*	= Melt reduced density
ρ_b^*	= Bulk reduced density
η^*	= Dimensionless viscosity contrast
U_{mf}	= Minimum fluidization velocity
U_{inj}	= Injection velocity

Run n°	$\rho_m(h)$	$\rho_b(h)$	ρ^*	ρ_b^*	η^*	U_{mf}	U_{inj}
A1	2500	3012	0	-0.2048	1	2.956 10 ⁻⁴	6.268 10 ⁻³
A2	2500	3012	0	-0.2048	5	5.913 10 ⁻⁵	1.254 10 ⁻³
A3	2500	3012	0	-0.2048	10	2.957 10 ⁻⁵	6.268 10 ⁻⁴
A4	2500	3012	0	-0.2048	50	5.913 10 ⁻⁶	1.254 10 ⁻⁴
A5	2500	3012	0	-0.2048	100	2.957 10 ⁻⁶	6.268 10 ⁻⁵
A6	2450	2994	0.02	-0.1976	1	3.141 10 ⁻⁴	6.660 10 ⁻³
A7	2450	2994	0.02	-0.1976	5	6.283 10 ⁻⁵	1.332 10 ⁻³
A8	2450	2994	0.02	-0.1976	10	3.141 10 ⁻⁵	6.660 10 ⁻⁴
A9	2450	2994	0.02	-0.1976	50	6.283 10 ⁻⁶	1.332 10 ⁻⁴
A10	2450	2994	0.02	-0.1976	100	3.141 10 ⁻⁶	6.660 10 ⁻⁵
A11	2550	3030	-0.02	-0.212	1	2.772 10 ⁻⁴	5.876 10 ⁻³
A12	2550	3030	-0.02	-0.212	5	5.544 10 ⁻⁵	1.175 10 ⁻³
A13	2550	3030	-0.02	-0.212	10	2.772 10 ⁻⁵	5.876 10 ⁻⁴
A14	2550	3030	-0.02	-0.212	50	5.544 10 ⁻⁶	1.175 10 ⁻⁴
A15	2550	3030	-0.02	-0.212	100	2.772 10 ⁻⁶	5.876 10 ⁻⁵
A16	2200	2904	0.12	-0.1616	1	4.065 10 ⁻⁴	8.618 10 ⁻³
A17	2200	2904	0.12	-0.1616	5	8.130 10 ⁻⁵	1.724 10 ⁻³
A18	2200	2904	0.12	-0.1616	10	4.065 10 ⁻⁵	8.618 10 ⁻⁴
A19	2200	2904	0.12	-0.1616	50	8.130 10 ⁻⁶	1.724 10 ⁻⁴
A20	2200	2904	0.12	-0.1616	100	4.065 10 ⁻⁶	8.618 10 ⁻⁵
A21	2150	2886	0.14	-0.1544	1	4.250 10 ⁻⁴	9.010 10 ⁻³
A22	2150	2886	0.14	-0.1544	5	8.500 10 ⁻⁴	1.802 10 ⁻³
A23	2150	2886	0.14	-0.1544	10	4.250 10 ⁻⁵	9.010 10 ⁻⁴
A24	2150	2886	0.14	-0.1544	50	8.500 10 ⁻⁶	1.802 10 ⁻⁴
A25	2150	2886	0.14	-0.1544	100	4.250 10 ⁻⁶	9.010 10 ⁻⁵

Table 2: Variable parameters used in the set of simulations exploring the influence of the density and viscosity contrasts between the mush and the intrusion



Effect of the injection velocity: Comparison of the maximum height of the intrusion as a function of the dimensionless time. The maximum height is normalized by the initial mush layer thickness ($H^* = H_{max}/H_{bed}$). Each square represents the measured height of the intrusion in the simulation. Their colors depend on the injection velocities. All simulations uses the same density and viscosity contrasts, taken from simulation A25. For these conditions, the intruder is expected to emplace as an horizontal layer. The dashed, solid, and dotted curves represent the theoretical height of the intrusion for a vertical growth, a radial growth and a lateral spreading, respectively

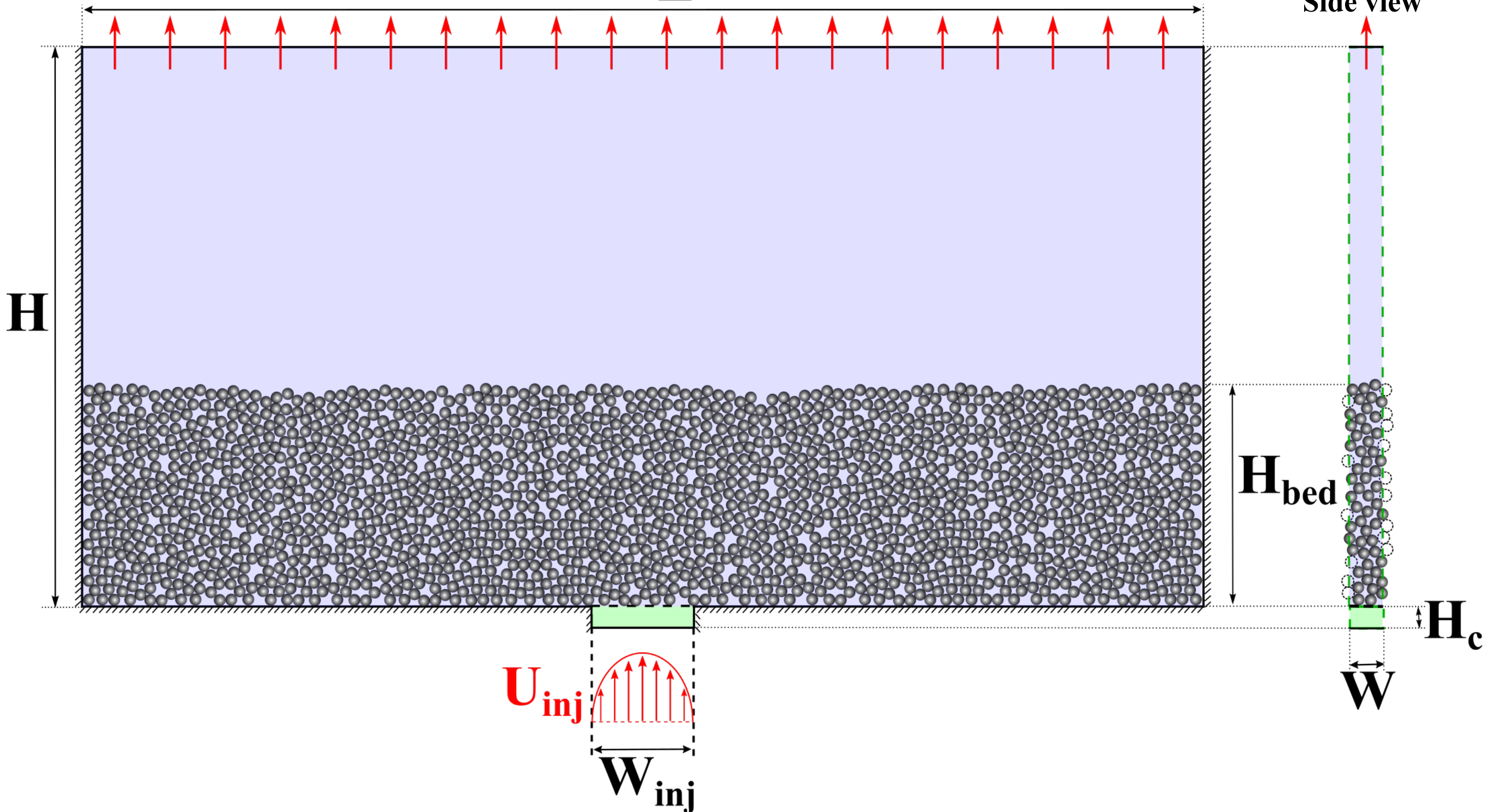


[Back to main slide](#)



Front view

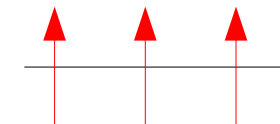
L



H = domain height (0.8m); L = domain length (1.6m); U_{inj} = injection superficial velocity; W_{inj} = injection width (0,1 m);

H_{bed} = mush layer height (0,3 m); W = domain width (0,05 m); H_c = conduit height (0,032 m).

Boundary conditions:



Pressure outflow



Cyclical



Mass inflow

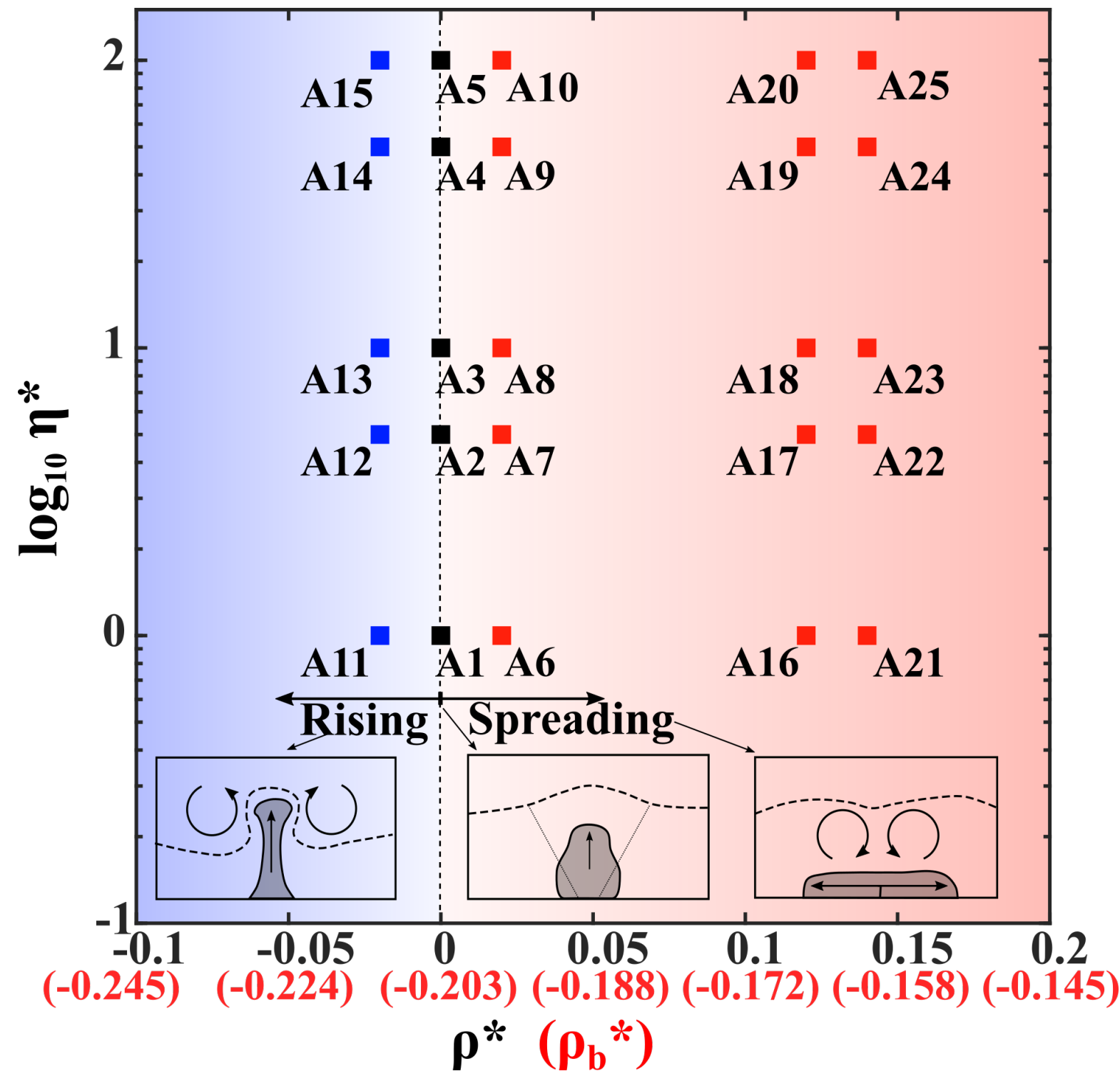


Non slip wall

[Back to main slide](#)

[Simulation parameters](#)

[Effect of viscosity contrast](#)

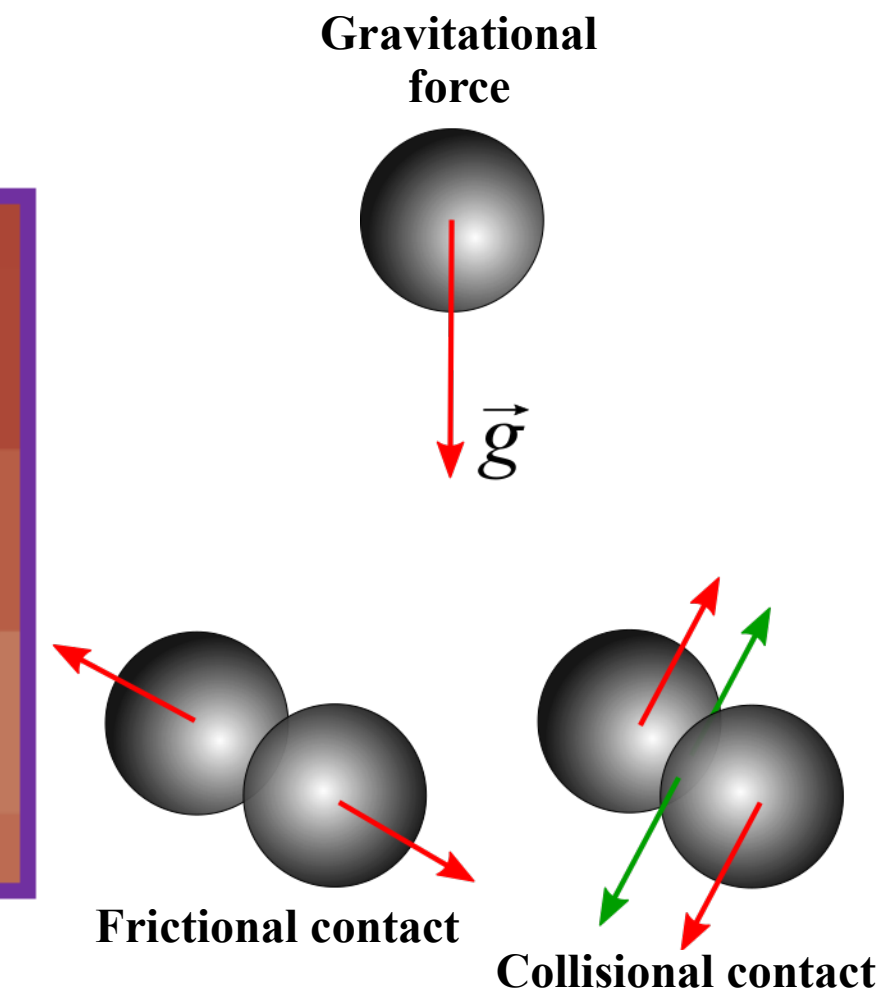
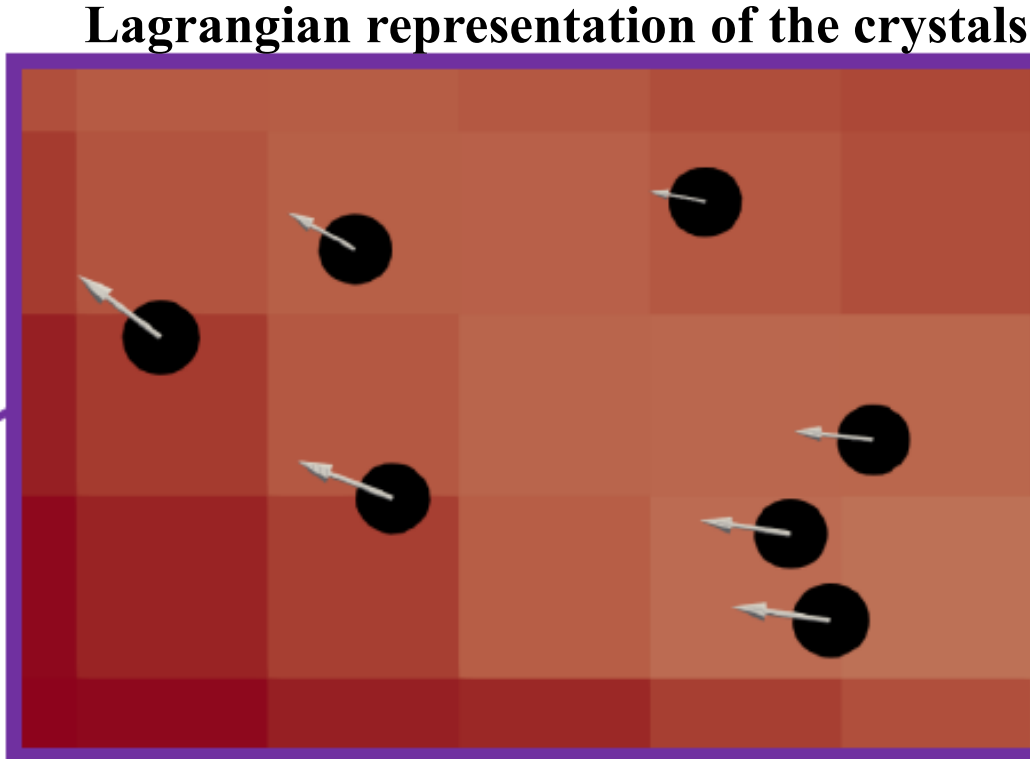
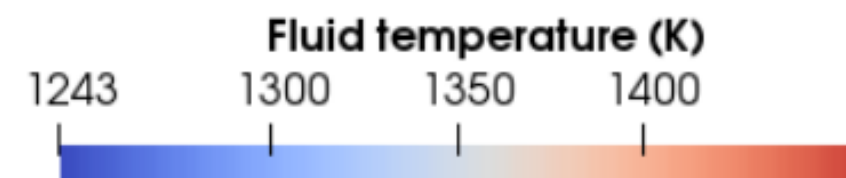
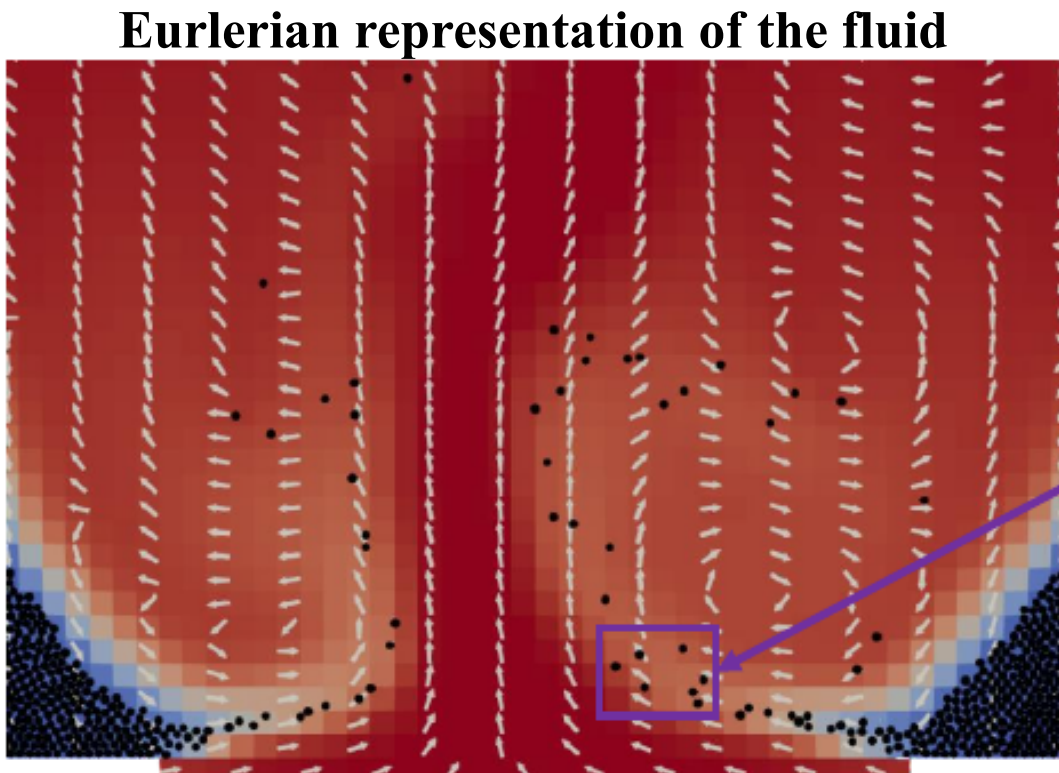


Influence of the density and viscosity contrasts ($U^*=22.1$): Each square represents a simulation. The red, blue and black colors indicate the occurrence of the lateral spreading, rising, and fluidization regimes, respectively. On the abscissa, the coordinates in black are for the melt reduced density and the red ones for the reduced bulk density.

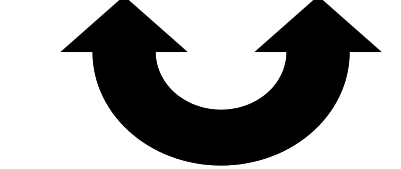
η^* = viscosity contrast ; ρ^* = reduced melt density ; ρ_b^* = reduced bulk density



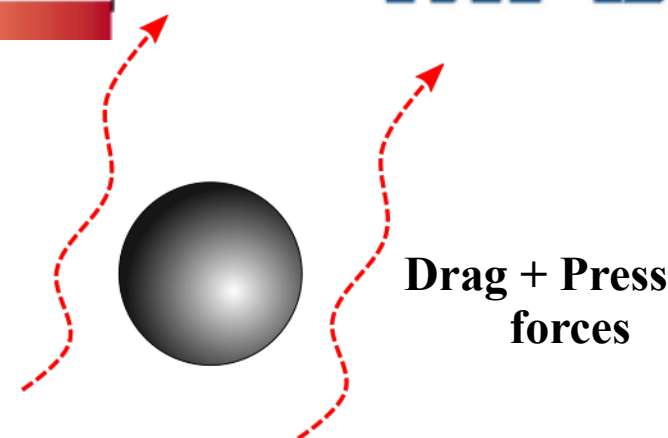
Overview of the numerical method



MFiX DEM

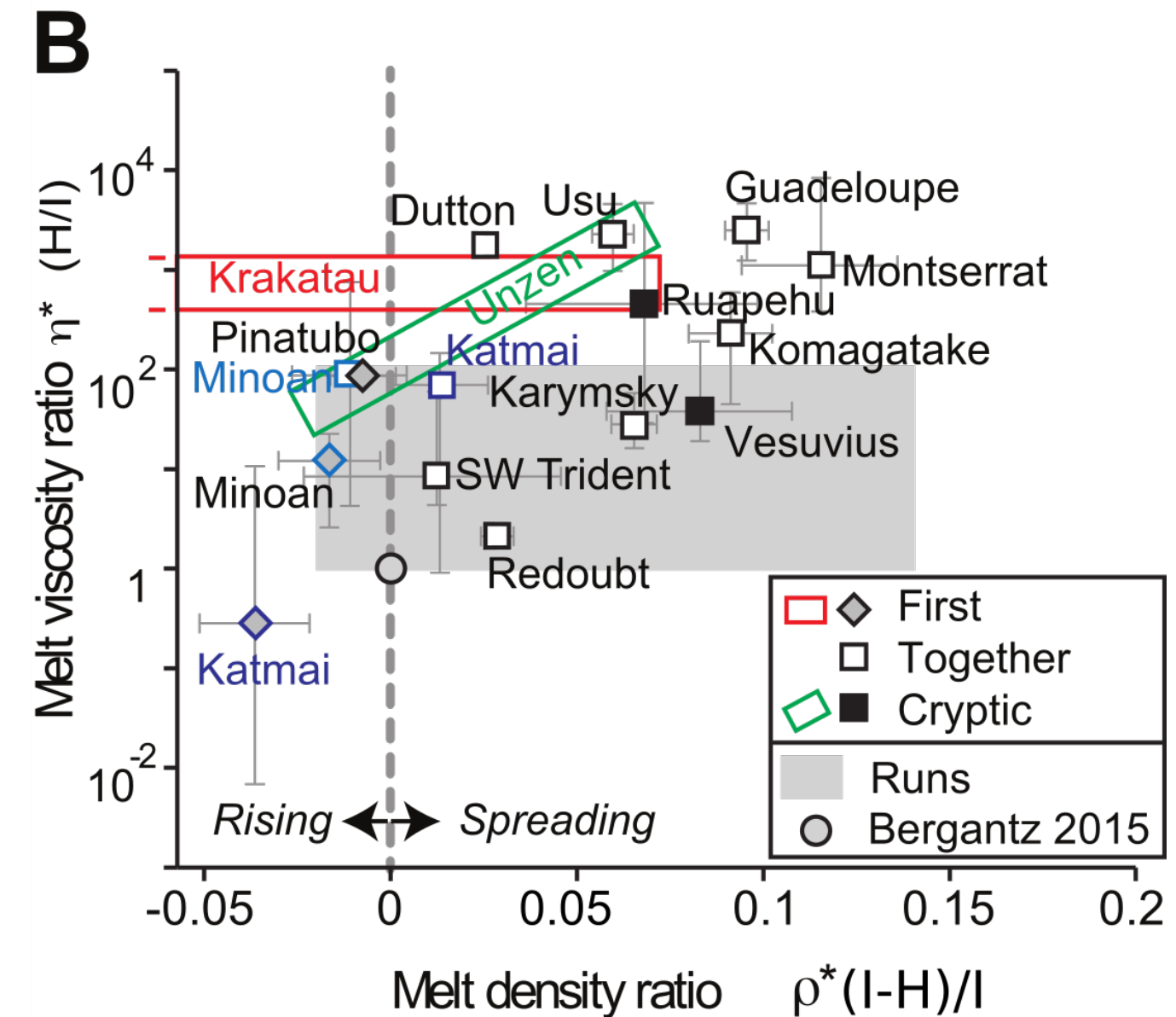
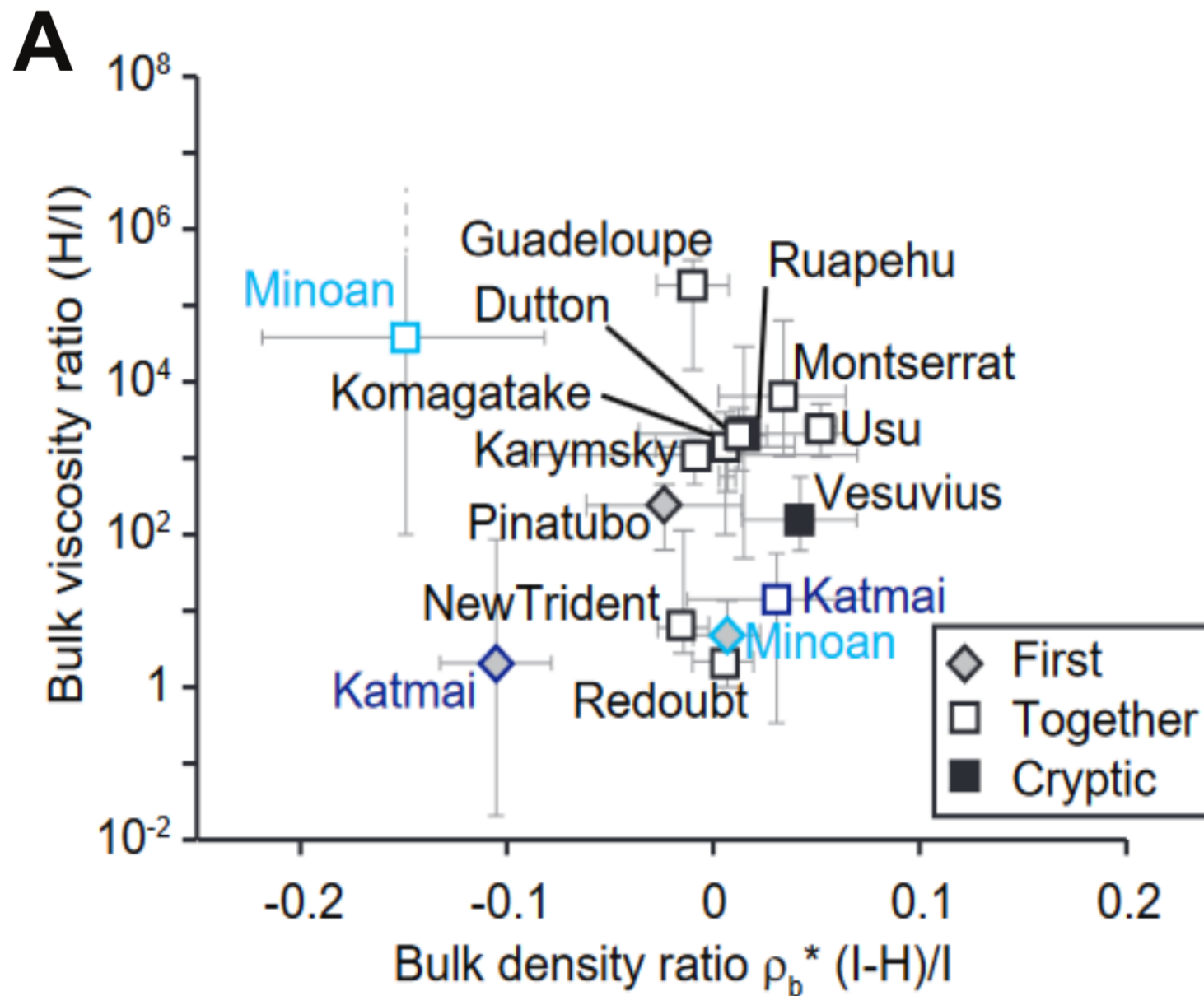


Momentum coupling =



Drag + Pressure
forces

We used an Eulerian-Lagrangian numerical model. For the fluid, the Navier-Stokes equations are solved (energy equation is neglected here) using a finite volume method. For each particle, the Newton's second law is solved to compute its motion with the external forces applied to it. We considered the gravitational, collisional, frictional, drag, and pressure forces. The two phases are four way coupled, meaning that they can exchange momentum through the drag force. Details of the model and equations can be found in Garg et al. (2012), Syamlal (1998), Syamlal et al. (1993).



Comparison with eruptive sequences: [A] Ratios of bulk properties for the host and intruder magmas involved in 15 eruptions. The bulk viscosity ratio is that of the host over that of the intruder and the bulk density ratio is that of the difference between the intruder and the host over that of the intruder. Eruptions are sorted according to whether the intruder magma was erupted first (“First”), at the same time as (or mixed with) the host (“Together”), or fully mixed with the host (“Cryptic”). [B] Ratios of melt properties for the host and intruder magmas involved in 15 eruptions. The melt viscosity ratio is that of the host over that of the intruder and the melt density ratio is that of the difference between the intruder and the host over that of the intruder. Eruptions are sorted according to whether the intruder magma was erupted first (“First”), at the same time as (or mixed with) the host (“Together”), or fully mixed with the host (“Cryptic”). The gray area covers the runs done in this study and the cross marks the parameters used in the numerical study of Bergantz et al. (2015). See <https://eartharxiv.org/hc4px/> for details regarding the special cases of Unzen and Krakatau.





Viscosity ratio $\eta^* = \frac{\eta(h)}{\eta(i)}$ Ratio of the host and intruded melt dynamic viscosities

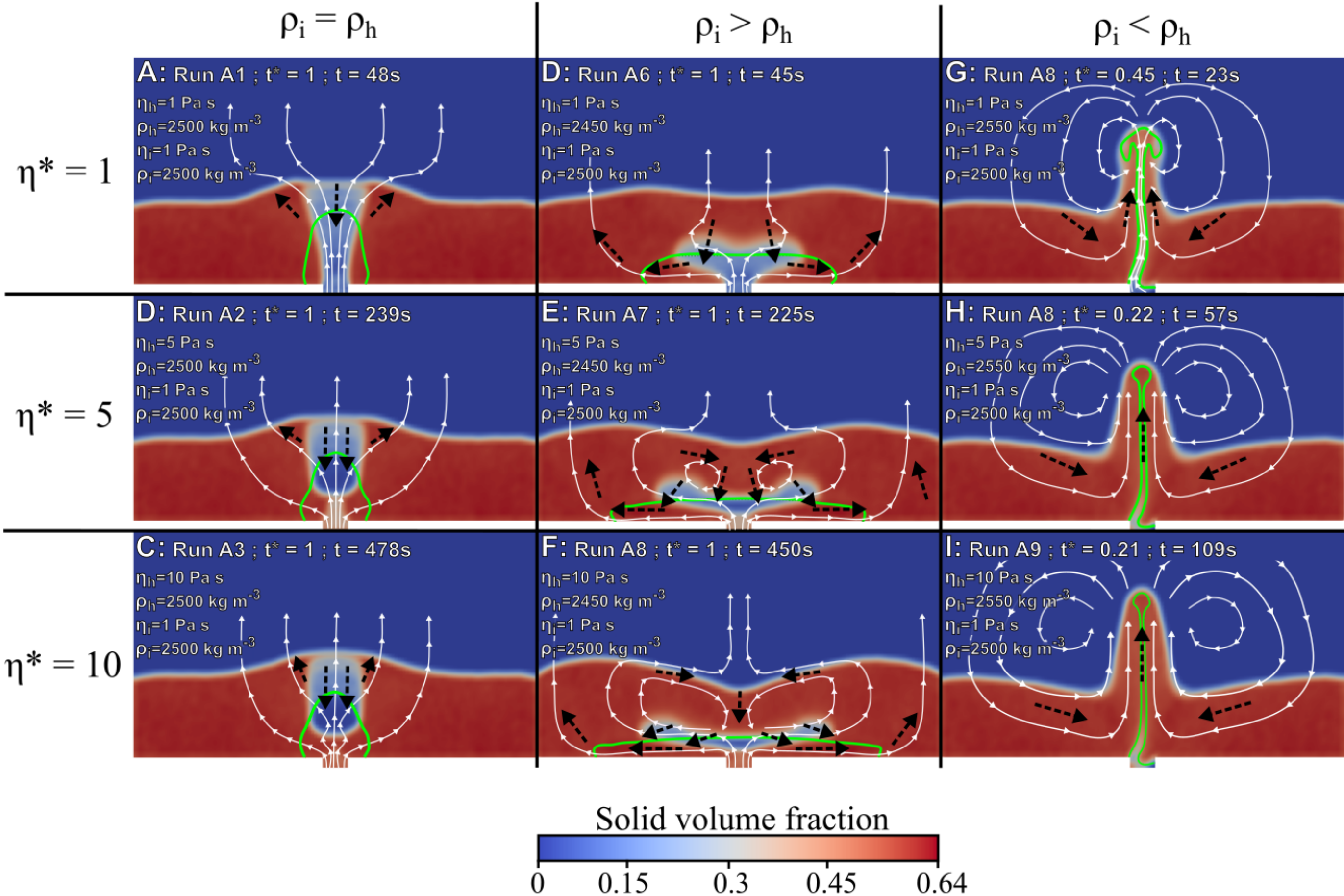
Reduced melt density $\rho^* = \frac{\rho(i) - \rho(h)}{\rho(i)}$ Comparison of intruded and host melt densities. Negative value indicates that the intruded melt is buoyant. Positive value indicates that the intruded melt is denser than the host one

Reduced bulk density $\rho_b^* = \frac{\rho(i) - [(1-\phi)\rho(h) + \phi\rho_c]}{\rho(i)}$ Comparison of intruded and host bulk densities. As the injected magma is crystal-free, we only included the host crystal volume fraction. Negative value indicates that the intruded magma is buoyant. Positive value indicates that the intruded magma is denser than the host one.

Dimensionless injection velocity $U^* = \frac{U_{inj}}{U_{mf}}$ Ratio of the injection superficial velocity and minimum fluidization velocity. The minimum fluidization velocity predicts at which injection rate the crystals starts to be entrained. This quantities is useful to scale the stress imposed by the intrusion on the mush layer. Two simulation with the same dimensionless injection velocity have the same stress imposed to the mush

Dimensionless time $t^* = \frac{t U_{inj}}{H_{bed}}$ This quantities is useful to scale the volume of intrusion injected in the simulations. Two simulations with the same dimensionless time have the same volume of intruded melt injected.

$\eta(h)$	= host melt viscosity
$\eta(i)$	= intrusion melt viscosity
$\rho(i)$	= intrusion melt density
$\rho(h)$	= host melt density
ρ_c	= crystals density
Φ	= crystal volume fraction
U_{inj}	= injection velocity
U_{mf}	= minimum fluidization velocity
t	= dimensional time
H_{bed}	= Mush layer thickness





ρ_c	= Crystal density
dp	= crystals diameters
H_{bed}	= Mesh layer thickness
W_{inj}	= Injection width
$\rho(i)$	= melt density in the intrusion
$\eta(i)$	= Viscosity of the melt phase in the intrusion
E	= Young modulus crystals
σ	= Poisson coefficient crystals
μ	= friction coefficients crystals
$\rho(h)$	= host melt density
$\rho_b(i)$	= bulk density of the host mush
ρ^*	= melt density contrast
ρ_b^*	= bulk density contrast
η^*	= dimensionless viscosity contrast
U_{mf}	= minimum fluidization velocity
U_{inj}	= Injection velocity

Parameter	Value or range
ρ_c	3300 kg m ⁻³
dp	4.5-5.5 mm
Nb crystals	208495
H_{bed}	0.3 m
W_{inj}	0.1 m
$\rho_m(1)$	2500 kg m ⁻³
$\eta(1)$	1 Pa s
E	2 10 ⁷ Pa
σ	0.32
μ	0.3

Table 1: Constant parameters used in the simulations

Run n°	$\rho_m(h)$	$\rho_b(h)$	ρ^*	ρ_b^*	η^*	U_{mf}	U_{inj}
A25	2150	2886	0.14	-0.1544	100	4.250 10 ⁻⁶	9.010 10 ⁻⁵
B1	2150	2886	0.14	-0.1544	100	4.250 10 ⁻⁶	4.250 10 ⁻³
B2	2150	2886	0.14	-0.1544	100	4.250 10 ⁻⁶	4.250 10 ⁻²
B3	2150	2886	0.14	-0.1544	100	4.250 10 ⁻⁶	4.250 10 ⁻¹
B4	2150	2886	0.14	-0.1544	100	4.250 10 ⁻⁶	4.250 10 ⁰

Table 2: Variable parameters used in the set simulations exploring the influence of the density and viscosity contrast between the mush and the intrusion

Back



CASE	Name	Xtal (vol%)	Minerals	Melt SiO ₂ (wt%)	Melt H ₂ O (wt%)	Melt density (kg/m ³)	Melt viscosity (Pa s)	T (°C)	P (MPa)	Ref
Unzen 1991	Dacite	34-35	Plag (0.8) Cpx (0.2)	75	8	2229-2239	1.3×10 ⁴ -1.4×10 ⁴	775	300	1
Vesuvius -79	White Pumice	31.6-40	Plag	53-57	sat.	2218-2300	2.4×10 ³ -3.0×10 ³	875-900	150 ^b	2
Guadeloupe 1530	Andesite	48.3-57.5	Plag (0.8) Px (0.2)	73-75	5.5-6	2189-2203	1.2×10 ⁴ -2.5×10 ⁴	825-875	135-200	3
Karymsky 1996	Andesite	25-32	Plag (0.8) Px (0.2)	63	sat.	2395-2378 ^a	8.9×10 ³ -13×10 ³ ^a	1023-1057	200 ^b	4
Ruapehu 1995	Andesite	24.5-42	Plag (0.66) Px (0.33)	62-70	1-1.5	2380-2438	2.9×10 ⁴ -4.7×10 ⁴	920-1030	40	5
Katmai 1912 – scenario 1	Andesite	30-45	Plag (0.8) Px (0.2)	67.6-74	usat-sat.	2274-2284	1.2×10 ⁴ -1.3×10 ⁴	920-970	75-120	6
	Dacite	30-45	Plag (0.8) Px (0.2)	79.1	usat-sat.	2189-2220	2.0×10 ⁵ -8.1×10 ⁵	850-910	60-25	
Katmai 1912 – scenario 2	Andesite	30	Plag (0.8) Px (0.2)	67.6	usat.	2274	1.2×10 ⁴	920	75	7
	Rhyolite	2	Plag	77	4	2225	1.7×10 ⁶	790	40	
Komagatake 1640	White Pumice	25-43.1	n.u.	74.7-76.1	3-4	2280-2300	4.4×10 ⁴ -2.9×10 ⁵ ^a	970-980	n.u.	8
Montserrat 1995	Andesite	35-45	Plag	75-80	4.8	2171-2160	3.7×10 ⁴ -8.4×10 ⁴	835-880	105-155	9
Redoubt 1990	Dacite	24-32	Plag	78.5-81	4	2164-2174	3.4×10 ⁴ -3.8×10 ⁴	840-950	100	10
Krakatau 1883	White Rhyodacite	7-15	Plag	70-74	4	2220-2400	3.1×10 ⁴ -3.4×10 ⁴	880-890	100-150	11
	Gray Dacite	4-12	Plag	66.5-75	4	2190-2200	1.3×10 ⁴ -1.4×10 ⁴	890-913	100-150	
Minoan – scenario 1	Rhyodacite	10-20	Plag	73.5-74	5-6	2222-2173	1.7×10 ⁴ -1.4×10 ⁵	845-860	200-250	12
Minoan – scenario 2	Andesite	55-100	Plag (0.8) CPx (0.2)	71-77	sat. ^b	2213-2231	5.9×10 ⁵ -1.3×10 ⁷	700-820	50	13
SW Trident 1953	Dacite	37-39	Plag (0.8) Px (0.2)	75	3.6	2190-2200	4.5×10 ⁴ -4.9×10 ⁴	890	90	14
Dutton 1989	Dacite	35	Plag (0.8) OPx (0.2)	78	sat.	2481-2491	1.4×10 ⁵ -1.5×10 ⁵	865	200 ^b	15
Pinatubo 1991	White Pumice	47	Plag (0.8) Hb (0.2)	76	6-6.5	2166	5.4×10 ⁴	750-800	155-200	16
	Tan Pumice	15-26	Plag (0.8) Hb (0.2)	73	6-6.5	2194	5.6×10 ⁴	750-800	155-200	
Usu 1663	Silicic magma	2.6-5.3	Plag (0.8) OPx (0.2)	74	n.u.	2210-2224	9.5×10 ⁴ -2.6×10 ⁵	750-800	n.u.	17

^a Calculated from bulk values given in the reference(s).^b Assumed value.

References are: 1) Holtz et al. (2005), Vetere et al. (2008)(andesite intruder), Browne et al. (2006)(basalt intruder); 2) Cioni et al. (1995), Scaillet et al. (2008); 3) Pichavant et al. (2018); 4) Izbekov et al. (2002), Izbekov et al. (2004), Eichelberger and Izbekov (2000); 5) Nakagawa et al. (1999), Nakagawa et al. (2002), Kilgour et al. (2013); 6) Eichelberger and Izbekov (2000), Coombs and Gardner (2001); 7) Hammer et al. (2002), Singer et al. (2016); 8) Takahashi and Nakagawa (2013); 9) Barclay et al. (1998), Murphy et al. (2000), Couch et al. (2001), Humphreys et al. (2010), Plail et al. (2018); 10) Wolf and Eichelbeger (1997), Nye et al. (1994), Swanson et al. (1994); 11) Camus et al. (1987), Self (1992), Mandeville et al. (1996); 12) Cottrell et al. (1999), Druitt et al. (1999), Cadoux et al. (2014), Flaherty et al. (2018); 13) Druitt (2014); 14) Coombs et al. (2000), Coombs et al. (2002); 15) Miller et al. (1999); 16) Pallister et al. (1992), Pallister et al. (1996), Bernard et al. (1996); 17) Tomiya and Takahashi (2005).